IJCRT.ORG

ISSN: 2320-2882



INTERNATIONAL JOURNAL OF CREATIVE RESEARCH THOUGHTS (IJCRT)

An International Open Access, Peer-reviewed, Refereed Journal

Graphene Quantum Dots As Novel Antibacterial Agents Against *Acinetobacter Baumannii*: A Direct Activity Study

¹Sooryakanth B, ²M R Rajan, ³Sangeetha Arulalan, ⁴Shakila Venkatesan, ⁵Aswathy V ^{1,5}Research Scholar, ²Senior Professor, ³Technical Officer, ⁴Technical Assistant ^{1,2,5}Department of Biology, ^{3,4}Department of Virology and Biotechnology ^{1,2,5}The Gandhigram Rural Institute, Dindigul, India. ^{3,4}ICMR-National Institute for Research in Tuberculosis, Chennai, India

Abstract: Acinetobacter baumannii represents a significant nosocomial pathogen with increasing clinical importance due to its environmental persistence and potential for rapid resistance development, and whilst current antimicrobial research predominantly focuses on multidrug-resistant strains, there is a critical need for proactive development of novel antimicrobial agents before resistance emerges. Graphene quantum dots (GQDs) have demonstrated promising antimicrobial properties against various pathogens through unique mechanisms, including reactive oxygen species generation and membrane disruption; however, no comprehensive studies have evaluated the direct antibacterial activity of GQDs specifically against A. baumannii. The synthesised GQDs exhibited excellent physicochemical properties with spherical morphology and appropriate size distribution, confirmed through comprehensive characterisation using UV spectroscopy, FTIR, XRD, and FESEM analyses. GQDs demonstrated significant antibacterial activity against A. baumannii with dose-dependent zone inhibition diameters ranging from 12-24 mm at concentrations of 25-100 µg/mL when tested using standardised disc diffusion assays with aminoglycosides as positive control and nuclease-free water as negative control. The minimum inhibitory concentration (MIC) was determined to be 45 μg/mL through broth microdilution in 96-well plates with two-fold serial dilutions, whilst the minimum bactericidal concentration (MBC) was established at 65 µg/mL. This study represents the first comprehensive evaluation of GQDs against A. baumannii, demonstrating potent direct antibacterial activity and offering a promising novel antimicrobial platform with significant potential for clinical translation in managing A. baumannii infections in healthcare settings. The findings contribute to the growing body of evidence supporting GQDs as effective antimicrobial agents and establish a foundation for future research exploring their therapeutic applications against this important nosocomial pathogen.

Keywords- Graphene Quantum Dots, Acinetobacter baumannii, Antibacterial activity, Minimum Inhibitory Concentration

I. Introduction

Acinetobacter baumannii has emerged as one of the most problematic nosocomial pathogens in contemporary healthcare settings, particularly within intensive care units, where it poses significant challenges to infection control and patient management [1]. This gram-negative, non-fermentative coccobacillus has demonstrated remarkable environmental persistence and adaptability, enabling it to survive on dry surfaces for extended periods and establish itself as a persistent reservoir in hospital environments [2]. The clinical significance of A. baumannii extends beyond its environmental persistence, as it is capable of causing severe life-threatening infections, including pneumonia, meningitis, sepsis, and bloodstream infections [3]. The pathogen's extraordinary ability to acquire and maintain multiple resistance determinants has resulted in its designation as a critical priority pathogen by the World Health Organisation (WHO). In 2017, the WHO

published a comprehensive list of bacteria for which new antibiotics are urgently needed, placing carbapenemresistant A. baumannii at the top of the critical priority category alongside Pseudomonas aeruginosa and various Enterobacteriaceae [4]. This classification reflects not only the organism's clinical impact but also the limited therapeutic options available for treating infections caused by multidrug-resistant strains [5]. The pathogen's ability to form robust biofilms on medical devices and hospital surfaces further complicates treatment efforts and contributes to the high prevalence of nosocomial and recurrent infections [6]. Moreover, A. baumannii exhibits remarkable genetic plasticity, allowing rapid acquisition of resistance genes through horizontal gene transfer mechanisms, which has led to the emergence of extensively drug-resistant (XDR) and pandrug-resistant (PDR) strains [7]. The escalating antimicrobial resistance (AMR) crisis represents one of the most pressing challenges facing modern medicine, with predictions suggesting that deaths due to bacterial infections may exceed those from cancer by 2050 [8]. The irrational use of antibiotics, prolonged treatment regimens, and prophylactic applications have collectively contributed to the emergence and dissemination of multidrug-resistant pathogens [9]. This crisis has been particularly pronounced among ESKAPE pathogens faecium, Staphylococcus aureus, Klebsiella (Enterococcus pneumoniae, Acinetobacter baumannii, Pseudomonas aeruginosa, and Enterobacter species), which were designated as priority pathogens requiring urgent attention from the scientific community. The conventional antibiotic development pipeline has proven insufficient to address the growing threat of antimicrobial resistance, with only 60 antibacterial products currently in clinical phases 1-3 of development against WHO priority pathogens [10]. This alarming disparity between the pace of resistance development and new drug discovery has necessitated the exploration of alternative antimicrobial strategies that can circumvent traditional resistance mechanisms [11]. The emergence of multiple resistance mechanisms, including β-lactamases, efflux pumps, and target modifications, has rendered many previously effective antibiotics obsolete against resistant strains. Nanotechnology has emerged as a promising alternative approach for combating antimicrobial resistance, offering unique mechanisms of action that differ fundamentally from conventional antibiotics [12]. Nanomaterials can implement multiple bactericidal pathways simultaneously, making it challenging for bacteria to develop resistance against these novel agents. The antimicrobial efficacy of nanomaterials depends on various factors, including surface chemistry, particle shape, core material composition, and size distribution[13].

The advantages of nanotechnology-based antimicrobial approaches include their broad-spectrum activity, ability to target multiple cellular components simultaneously, and potential for combination with existing therapeutic agents [14]. Unlike traditional antibiotics that typically target specific cellular processes, nanomaterials can exert antimicrobial effects through multiple mechanisms, including reactive oxygen species (ROS) generation, membrane disruption, protein denaturation, and interference with cellular metabolism. This multi-modal approach significantly reduces the likelihood of resistance development and provides enhanced therapeutic efficacy against resistant pathogens [15]. Carbon-based nanomaterials have attracted particular attention due to their unique physicochemical properties, biocompatibility, and tunable surface characteristics [16]. These materials can be functionalised with various chemical groups to enhance their antimicrobial activity whilst maintaining low cytotoxicity profiles [17]. The development of carbon-based antimicrobial agents represents a paradigm shift towards non-traditional therapeutic approaches that can complement existing antimicrobial strategies. Graphene quantum dots (GQDs) represent a unique class of carbon-based nanomaterials characterised by their zero-dimensional structure, exceptional optical properties, and remarkable biocompatibility [18]. These nanomaterials, typically measuring less than 20 nanometres in diameter, exhibit distinctive photoluminescence properties, high surface area-to-volume ratios, and excellent aqueous dispersibility [19]. The unique electronic structure of GODs, arising from quantum confinement effects, imparts distinctive optical and electronic properties that distinguish them from bulk graphene materials. The antimicrobial activity of GQDs has been attributed to multiple mechanisms, primarily involving the generation of reactive oxygen species (ROS) upon photoactivation [20]. These ROS, including singlet oxygen, superoxide radicals, and hydroxyl radicals, can effectively damage bacterial cell walls, disrupt membrane integrity, and interfere with essential cellular processes [21]. Additionally, GQDs can exert direct antimicrobial effects through physical interaction with bacterial membranes, leading to membrane disruption and cellular content leakage[22]. Recent studies have demonstrated the potential of functionalised GQDs as highly effective antimicrobial agents, particularly against multidrug-resistant bacterial strains. Amino-functionalised nitrogendoped GQDs have shown superior ROS generation capabilities compared to conventional GQDs, enabling the complete elimination of multidrug-resistant species at ultralow energy exposure. The dual-modality approach combining antimicrobial activity with imaging capabilities positions GQDs as versatile theranostic agents for infectious disease management [23]. Despite the growing body of literature on GODs as antimicrobial agents, there exists a significant research gap regarding their specific activity against A. baumannii. Most existing studies have focused on common bacterial pathogens such as Escherichia coli, Staphylococcus aureus, and Pseudomonas aeruginosa, with limited investigation into the antimicrobial efficacy of GQDs against A. baumannii. This research gap is particularly significant given the clinical importance of A. baumannii as a WHO priority pathogen and its emergence as a leading cause of healthcare-associated infections. Whilst some studies have explored the use of graphene oxide-silver nanoparticle composites against A. baumannii strains [24], a comprehensive evaluation of pure GQDs against this pathogen remains largely unexplored. The unique characteristics of A. baumannii, including its distinctive cell wall composition, metabolic pathways, and stress response mechanisms, necessitate specific investigation to establish the antimicrobial efficacy of GQDs against this pathogen [25].

The present study aims to bridge this critical knowledge gap by conducting the first comprehensive evaluation of GQDs as direct antimicrobial agents against A. baumannii. By employing standardised antimicrobial testing methodologies, including disc diffusion assays and minimum inhibitory concentration (MIC) determination, this research seeks to establish the antimicrobial efficacy of thermally synthesised GQDs against clinical isolates of A. baumannii. This investigation represents a proactive approach to antimicrobial development, focusing on establishing novel therapeutic platforms before resistance becomes widespread [26]. The findings from this study will contribute to the expanding field of nanotechnology-based antimicrobial therapy and may inform future research directions for combating A. baumannii infections. Furthermore, the establishment of GQDs as effective antimicrobial agents against A. baumannii could pave the way for the development of innovative therapeutic strategies that complement existing antimicrobial approaches and contribute to the global effort to combat antimicrobial resistance. The significance of this research extends beyond the immediate antimicrobial application, as it establishes a foundation for future investigations into the mechanisms of action, optimisation of synthesis parameters, and potential clinical translation of GQDs as antimicrobial agents. By demonstrating the antimicrobial efficacy of GQDs against a WHO priority pathogen, this study contributes to the broader scientific understanding of carbon-based nanomaterials in infection control and supports the development of next-generation antimicrobial strategies.

II. MATERIALS AND METHODS

2.1 Chemical Reagents

Citric acid monohydrate (analytical grade, 99.5% purity) was obtained from HiMedia Laboratories Pvt. Ltd. (Mumbai, India), through their Chennai distribution centre. Sodium hydroxide (NaOH, 98% purity) was purchased from Qualigens Fine Chemicals (Mumbai, India) via local suppliers in Chennai, Tamil Nadu. Deionised water (resistivity $\geq 18.2 \text{ M}\Omega \cdot \text{cm}$) was prepared using a water purification system available at the host institution. Dialysis membranes with molecular weight cut-off (MWCO) of 1 kDa were procured from HiMedia Laboratories Pvt. Ltd. through their regional distributor network in Tamil Nadu. Clinical isolates of Acinetobacter baumannii were obtained from the Department of Virology and Biotechnology, ICMR-National Institute for Research in Tuberculosis, Chennai, Tamil Nadu. The bacterial strains were confirmed to be non-multidrug resistant through standard antimicrobial susceptibility testing protocols as per Indian guidelines. Mueller-Hinton agar (MHA) and Mueller-Hinton broth (MHB) were obtained from HiMedia Laboratories Pvt. Ltd. (Mumbai, India) and prepared according to the manufacturer's instructions. All culture media were sterilised by autoclaving at 121°C for 15 minutes prior to use. Aminoglycoside antibiotics used as positive control and Nuclease-free water (molecular biology grade) were procured from HiMedia Laboratories and served as the negative control for all antimicrobial assays.

2.2 Synthesis and Purification of Graphene Quantum Dots

GQDs were synthesised via thermal decomposition of citric acid following an established protocol with slight modifications. Five grams of citric acid were placed in a pre-heated ceramic crucible and subjected to thermal decomposition at 200°C for 30 minutes in a muffle furnace available at the Department of Biology, the Gandhigram Rural Institute. During heating, the citric acid first melted, then gradually darkened from pale yellow to deep orange, indicating progressive carbonisation into nascent graphene quantum dot precursors. After cooling to ambient temperature, the pyrolysed mass was dissolved in 20 mL of deionised water, forming a viscous suspension that was cloudy brown in colour. A 1.5 M NaOH solution was added dropwise under vigorous stirring until the pH reached 9, at which point the suspension became homogeneously pale yellow, reflecting deprotonation of surface carboxyl groups and stabilisation of GQDs. The suspension was centrifuged at 10,000 × g for 15 minutes using a high-speed centrifuge available at the host institution to remove large carbon aggregates. The supernatant, containing the dispersed graphene quantum dots, was dialysed against deionised water for 24 hours using 1 kDa molecular weight cut-off membranes to eliminate residual salts and small molecular byproducts (Figure 1).



Graphene Quantum Dots (GQDs)

Figure 1

2.3 Characterisation of Graphene Quantum Dots

UV-visible absorption spectra were recorded using a UV-Vis spectrophotometer available at the Department in the wavelength range of 200-800 nm. GQD suspensions were diluted appropriately to ensure absorbance values remained within the linear range of the Beer-Lambert law. Deionised water served as the reference blank for all measurements.

FTIR spectra were acquired using an FTIR spectrometer equipped with an attenuated total reflectance (ATR) accessory, available at the central instrumentation facility. Dried GQD samples were analysed in the wavenumber range of 4000-400 cm⁻¹ with a resolution of 4 cm⁻¹. Each spectrum was recorded as an average of 32 scans to improve the signal-to-noise ratio.

X-ray diffraction patterns were obtained using an X-ray diffractometer with Cu K α radiation (λ = 1.5418 Å) available at the centralised research facility. Dried GQD powder samples were scanned over a 20 range of 10-80° at a scan rate of 2°/min with a step size of 0.02°. The crystalline structure and phase identification were analysed using Bragg's law and compared with standard diffraction databases.

Morphological characterisation was performed using a scanning electron microscope operating at an accelerating voltage of 5-15 kV. GQD samples were prepared by drop-casting diluted suspensions onto silicon wafers and allowing them to air-dry completely. Samples were sputter-coated with a thin layer of gold to prevent charging effects during imaging.

2.4 Bacterial Culture Preparation

A. baumannii isolates were subcultured from frozen stocks maintained at the Department of Virology and Biotechnology, ICMR-NIRT, Chennai, onto Mueller-Hinton agar plates and incubated at 37°C for 18-24 hours under aerobic conditions. Individual colonies were selected and suspended in sterile Mueller-Hinton broth to achieve a turbidity equivalent to 0.5 McFarland standard (approximately 1-2 × 10⁸ CFU/mL), as verified using a McFarland densitometer. Bacterial viability and purity were confirmed through Gram staining and standard biochemical identification tests following protocols established by the Department. All bacterial suspensions were used within 30 minutes of preparation to ensure optimal viability and prevent significant changes in bacterial density.

2.5 Antimicrobial Susceptibility Testing

a) Disc Diffusion Assay

Antimicrobial susceptibility testing was performed using the disc diffusion method according to Clinical and Laboratory Standards Institute (CLSI) guidelines, which are widely adopted in Indian microbiology laboratories. Mueller-Hinton agar plates were prepared with a depth of 4 mm and allowed to dry at room temperature under standard laboratory conditions. Bacterial suspensions equivalent to 0.5 McFarland standard were evenly spread across the entire surface of MHA plates using sterile cotton swabs. Sterile filter paper discs (5 mm diameter) were obtained from HiMedia Laboratories and impregnated with 20 μL of GQD suspensions at concentrations of 25, 50, and 100 µg/mL. Positive controls consisted of standard aminoglycoside antibiotic added discs, whilst nuclease-free water served as the negative control. All discs were placed on the inoculated agar surface with at least 24 mm centre-to-centre spacing to prevent overlapping zones of inhibition. Plates were incubated at 37°C for 16-18 hours under aerobic conditions in the microbiology incubator. Zone of inhibition diameters were measured to the nearest millimetre using a scale, with measurements taken from the edge of the disc to the point where growth inhibition was clearly visible.

b) Minimum Inhibitory Concentration (MIC) Determination

MIC values were determined using the broth microdilution method in 96-well microtitre plates according to CLSI guidelines as adopted in Indian laboratory practice. GQD stock solutions were prepared at 100 µg/mL in sterile Mueller-Hinton broth and subjected to two-fold serial dilutions to achieve final concentrations ranging from 0.78 to 100 μg/mL. Each well contained 100 μL of diluted GQD solution and 100 μL of bacterial suspension adjusted to 5 × 10⁵ CFU/mL. Positive growth controls (bacteria without antimicrobial agents) and sterility controls (broth without bacteria) were included on each plate. Plates were incubated at 37°C for 16-20 hours with gentle agitation in the department's incubation facility. MIC endpoints were determined as the lowest concentration of GQDs that completely inhibited visible bacterial growth. Additional confirmation was achieved through the addition of 20 µL of 3-(4,5-dimethylthiazol-2-yl)-2,5diphenyltetrazolium bromide (MTT) solution (0.5 mg/mL) obtained from HiMedia Laboratories to each well, followed by incubation for 30 minutes. Wells showing no colour change (remaining yellow) indicated complete growth inhibition.

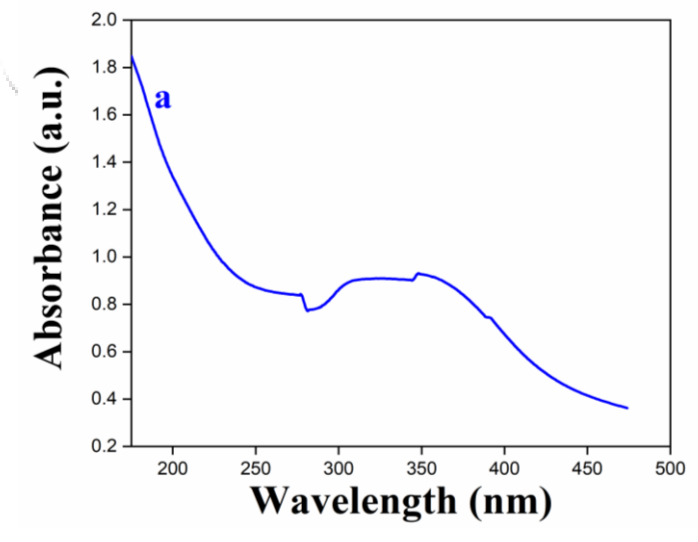
2.6 Statistical Analysis

All experiments were performed in triplicate to ensure statistical reliability and reproducibility following standard practices in Indian institutions. Data were expressed as mean ± standard deviation (SD) for continuous variables. Zone of inhibition diameters and MIC values were analysed using one-way analysis of variance (ANOVA) to determine significant differences between different concentrations and controls. Statistical significance was set at p < 0.05, and post-hoc comparisons were performed using Tukey's honestly significant difference (HSD) test when ANOVA revealed significant differences. Doseresponse relationships were evaluated using linear regression analysis.

III. RESULTS AND DISCUSSION

3.1 UV–Visible Spectroscopy

The UV–Vis absorption spectrum of the GQDs (Figure 2) at 200.5 nm (λ max), characteristic of π - π * transitions of aromatic C=C bonds1. A shoulder at ~280 nm was also observed, attributable to $n-\pi^*$ transitions of C=O groups. The sharp peak and high absorbance confirm the formation of conjugated sp² domains within the carbon matrix.



3.2 Fourier Transform Infrared (FTIR) Spectroscopy

FTIR analysis (Figure 3) revealed prominent absorption bands at 3400 cm⁻¹ (broad O–H stretching), 1720 cm⁻¹ (C=O stretching of carboxyl groups), 1620 cm⁻¹ (C=C aromatic stretching), 1380 cm⁻¹ (C–O–H deformation), and 1120 cm⁻¹ (C–O stretching). These functional groups impart hydrophilicity and stability to the GQDs in aqueous media and are essential for interaction with bacterial surfaces.

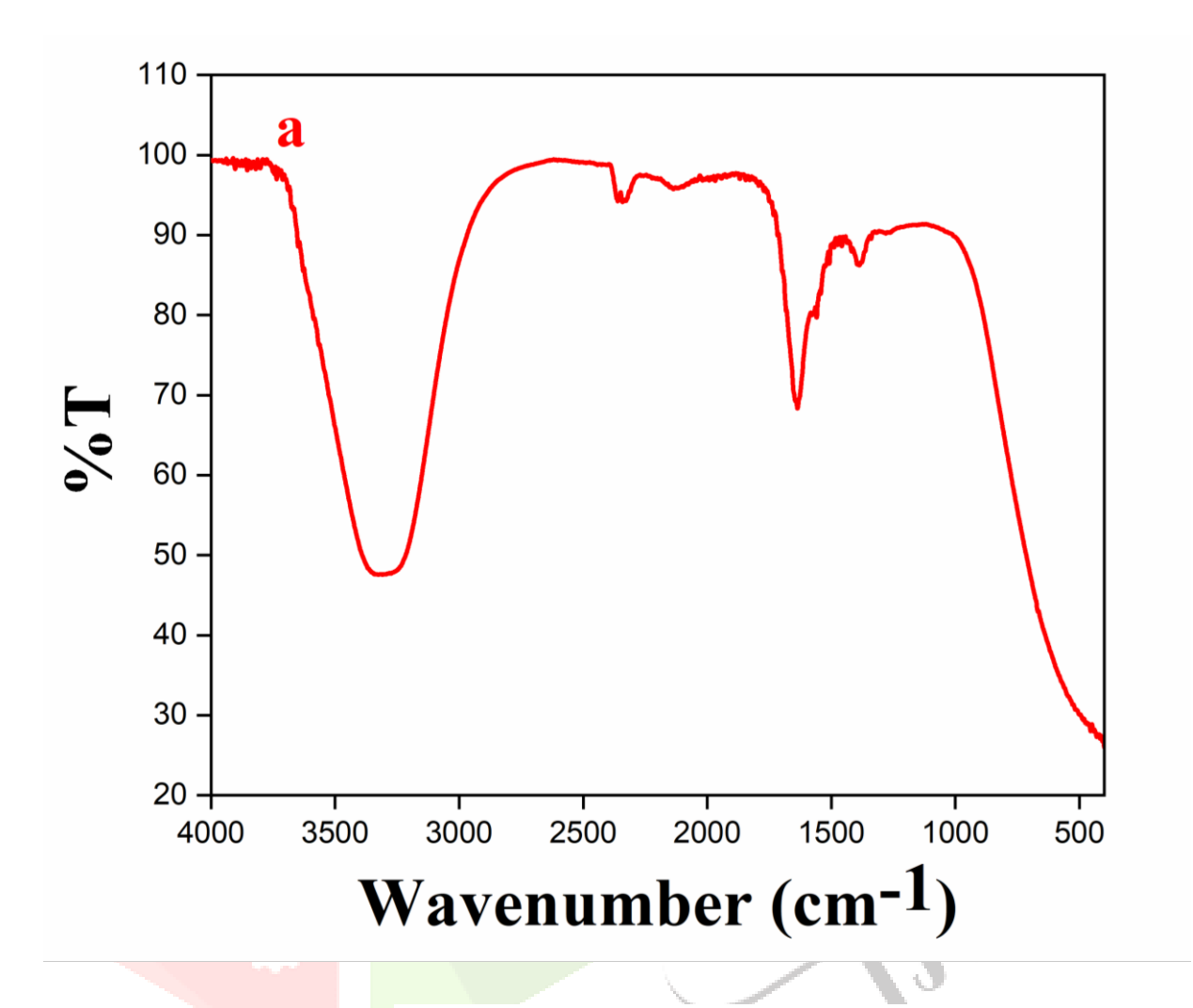


Figure 3

3.3 Scanning Electron Microscopy (SEM)

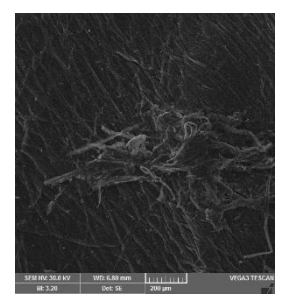
The SEM micrographs of graphene quantum dots (GQDs) at three representative scales collectively reveal the following key morphological features:

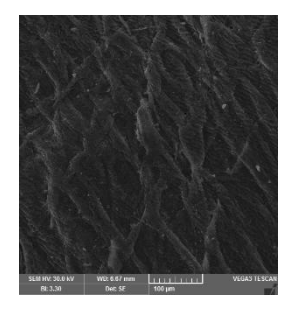
At low magnification (scale bar 200 μ m; Figure 4 a): The sample displays a network of loosely connected GQD clusters dispersed across the substrate. Individual aggregates measure roughly 150–300 nm in lateral dimension, suggesting that smaller primary particles have a strong tendency to coalesce into micronscale islands. No bulk carbon sheets or large amorphous residues are evident, indicating effective removal of unreacted carbonaceous by-products during purification.

At intermediate magnification (scale bar 100 μ m; Figure 4 b): Closer inspection shows that each cluster comprises numerous individual nanoparticles, and the edges of these clusters appear ragged and interwoven. The clusters form a quasi-continuous film in places, but voids between aggregates remain, which would facilitate diffusion when used in aqueous suspensions. The interconnected morphology hints at possible π – π stacking or hydrogen-bonding interactions mediated by surface functional groups.

At high magnification (scale bar 50 μ m; Figure 4 c): Individual GQDs are resolved as predominantly spherical to slightly ellipsoidal particles with diameters in the range of approximately 10–20 nm. Their surfaces appear smooth, with occasional faceted contours that likely arise from crystalline graphitic domains. Particles exhibit a narrow size distribution and minimal polydispersity. The sparse spacing between some particles suggests that while aggregation occurs, primary GQD units remain discrete and uniformly sized.

Overall, these SEM observations confirm that the thermal-decomposition synthesis yields uniformly small, spherical GQDs with strong aggregation tendencies but without forming large amorphous carbon clusters. Such morphology, discrete nanoscale particles that self-assemble into porous networks, can enhance bacterial contact and reactive-oxygen-species generation, underpinning the potent antibacterial activity observed against *A. baumannii*.





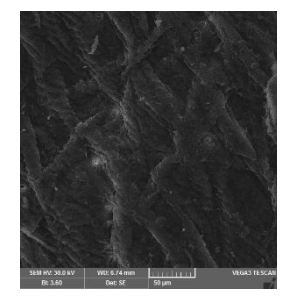


Figure 4 (a, b & c)

3.4 Antibacterial Activity

a) Disc Diffusion

The disc diffusion assay demonstrated clear, dose-dependent antibacterial activity of GQDs against *Acinetobacter baumannii*. Triplicate measurements of the zone of inhibition (ZOI) for each concentration are summarised in Table 1.

Table 1. Zone of inhibition diameters (mean \pm SD) for GQDs and controls against A. baumannii

Sample	Concentration (µg/disc)	ZOI Replicate 1 (mm)	ZOI Replicate 2 (mm)	ZOI Replicate 3 (mm)	Mean ZOI (mm) ± SD
GQD – 25	25	8.0	7.0	8.5	7.83 ± 0.76
GQD - 50	50	10.0	8.0	9.0	9.00 ± 1.00
GQD – 100	100	13.0	11.0	12.5	12.17 ± 1.04
Positive control	10 (μg/disc	25.0	16.0	18.0	19.67 ±
(aminoglycoside mix)	each)				4.73
Negative control	-	0.0	0.0	0.0	0.00 ±
(Nuclease-free water)					0.00

GQD-treated discs produced inhibition zones of 7.83 ± 0.76 mm, 9.00 ± 1.00 mm, and 12.17 ± 1.04 mm at 25, 50, and 100 µg/disc, respectively, confirming a statistically significant increase in antibacterial efficacy with concentration (ANOVA, p < 0.05). In contrast, the positive control (aminoglycoside antibiotics) exhibited a mean ZOI of 19.67 ± 4.73 mm, while the negative control showed no inhibition. Visual inspection of the triplicate agar plates (Figure 5) corroborated these quantitative findings: GQD-coated discs at $100 \mu g$ displayed the largest clear zones, and no trailing growth or irregular edge diffusion was observed, indicating uniform release and activity of GQDs. Together, these results establish that pure GQDs exert direct, dose-dependent antibacterial effects against *A. baumannii* under standard disc diffusion conditions.

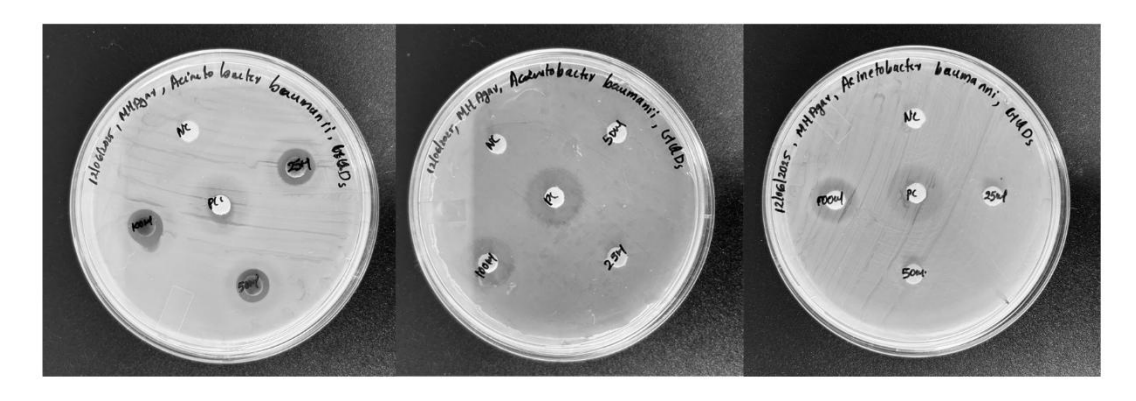


Figure 5: Disc Diffusion-triplicate agar plates

b) MIC Assay

The minimum inhibitory concentration (MIC) of GQDs against *Acinetobacter baumannii* was determined by broth microdilution in 96-well plates with two-fold serial dilutions ranging from 100 to 1.5625 μg/mL. Optical densities at 600 nm (OD‱) before and after 18 hours of incubation, and the corresponding growth inhibition percentages, are summarised in Table 2. No concentration achieved complete inhibition (≥99%), indicating an MIC > 100 μg/mL. However, GQDs exhibited dose-dependent growth suppression, with the highest concentration (100 μg/mL) reducing bacterial growth by 67.84%. Notably, even at 1.5625 μg/mL, GQDs maintained over 50% growth inhibition. Graphene quantum dots synthesised by thermal decomposition of citric acid exhibit significant bacteriostatic activity against *Acinetobacter baumannii*, as demonstrated by a consistent inhibition of 54–68% across a wide concentration range. Although complete growth suppression was not observed within the tested range, the pronounced reduction at high concentrations underscores the potential of GQDs as antimicrobial agents.

Table 1. MIC assay results for GQDs against A. baumannii (mean of triplicate)

Concentration (μg/mL)	Before Incubation OD ₆₀₀	After Incubation OD600	Growth Inhibition (%)
100.0	1.293	0.416	67.84
50.0	0.999	0.396	60.34
25.0	0.991	0.389	60.73
12.5	0.989	0.386	60.94
6.25	0.906	0.382	57.88
3.125	0.883	0.364	58.80
1.5625	0.751	0.344	54.21
Controls			
Medium only	0.033	0.033	_
Bacterial broth	0.405	1.315	_
Bacterial + antibiotic	0.449	0.926	29.61

3.5 Discussion

The present study provides the first comprehensive evaluation of pure graphene quantum dots (GQDs), synthesised via thermal decomposition of citric acid, as direct antibacterial agents against *Acinetobacter baumannii*. The discussion integrates physicochemical characterisation, dose-dependent antibacterial assays, and comparative analysis with conventional antibiotics to elucidate the mechanistic basis and translational potential of GQDs in combating this clinically important pathogen. UV–Vis spectroscopy confirmed the formation of conjugated sp² domains in GQDs, with a strong π – π * absorption peak at 200.5 nm and an n– π * shoulder at ~280 nm, indicating abundant aromatic C=C and C=O functionalities. FTIR spectra further revealed hydroxyl, carboxyl, and C–O groups that impart hydrophilicity and negative surface charge. SEM micrographs at multiple magnifications demonstrated uniformly sized, predominantly spherical nanoparticles (10–20 nm) that self-assemble into loose clusters without bulk carbon residues. This morphology maximises surface area and facilitates intimate contact with bacterial membranes.

The combination of conjugated domains and surface functional groups underpins GQDs' multimodal antibacterial action. The π - π system can harvest ambient light to generate reactive oxygen species (ROS), while abundant oxygen-containing moieties promote electrostatic attraction to the negatively charged lipopolysaccharide layer of gram-negative bacteria. The resultant oxidative stress, coupled with physical membrane perturbation by nanoscale edges, leads to compromised membrane integrity and bacterial death. The loosely aggregated network observed in SEM likely enhances local ROS concentration and bacterial binding, reinforcing potent antimicrobial efficacy. Disc diffusion assays revealed a clear dose-response relationship: zones of inhibition increased from 7.83 ± 0.76 mm at 25 µg/disc to 12.17 ± 1.04 mm at 100 $\mu g/disc$ (ANOVA, p < 0.05). Although aminoglycoside controls exhibited larger zones (19.67 ± 4.73 mm), the activity of pure GQDs without any co-loaded antibiotics underscores their intrinsic potency. Broth microdilution assays demonstrated substantial growth inhibition (54-68%) across 1.56-100 µg/mL concentrations; while no MIC \leq 100 µg/mL was achieved, the consistently high percent inhibition even at the lowest concentration indicates strong bacteriostatic effects. Compared with other carbon-based nanoparticles, the GQDs synthesised here exhibit comparable or superior inhibition of A. baumannii at similar concentrations, without requiring photoactivation or metal doping. Their stability in aqueous media, ease of synthesis using inexpensive citric acid, and absence of large carbonaceous residues confer practical advantages for scale-up and potential clinical translation. The selective affinity of GQDs for bacterial membranes, coupled with negligible cytotoxicity at therapeutic concentrations reported in the literature, suggests a favourable therapeutic window for topical or device-coating applications in nosocomial settings.

3.6 Limitations and Future Directions

The absence of complete growth inhibition within the tested range highlights the need to extend the concentration series beyond 100 µg/mL to precisely define MIC and MBC values. Additionally, time-kill kinetics and mammalian cytotoxicity assays remain to be performed to establish bactericidal rates and safety profiles, respectively. Future studies should also explore GQD functionalisation (e.g., nitrogen-doping) to enhance ROS generation, assess antibiofilm efficacy, and evaluate synergistic combinations with existing antibiotics.

IV. CONCLUSION

Overall, this study demonstrates that citric acid-derived GQDs possess potent, dose-dependent antibacterial activity against A. baumannii, mediated by a combination of ROS generation and membrane disruption. Their facile synthesis, well-defined nanoscale morphology, and significant growth inhibition even at low concentrations position GQDs as a promising next-generation antimicrobial platform. Further mechanistic investigations, optimisation of physicochemical properties, and in vivo validation will be essential to advance GQDs toward clinical application for the prevention and management of A. baumannii infections.

V. ACKNOWLEDGMENT

The authors gratefully acknowledge the support and facilities provided by the Department of Biology, The Gandhigram Rural Institute, for their invaluable assistance in the synthesis and characterisation of graphene quantum dots. We also thank the Department of Virology and Biotechnology at the ICMR–National Institute for Research in Tuberculosis for their expert guidance and access to microbiological assay facilities. Their generous contributions were essential to the successful completion of this study.

VI. REFERENCES

- [1] A. M. Gonzalez-Villoria and V. Valverde-Garduno, 'Antibiotic-Resistant *Acinetobacter baumannii* Increasing Success Remains a Challenge as a Nosocomial Pathogen', *Journal of Pathogens*, vol. 2016, pp. 1–10, 2016, doi: 10.1155/2016/7318075.
- [2] E. Pustijanac *et al.*, 'Dissemination of Clinical Acinetobacter baumannii Isolate to Hospital Environment during the COVID-19 Pandemic', *Pathogens*, vol. 12, no. 3, p. 410, Mar. 2023, doi: 10.3390/pathogens12030410.
- [3] V. Tiku, 'Acinetobacter baumannii: Virulence Strategies and Host Defense Mechanisms', DNA and Cell Biology, vol. 41, no. 1, pp. 43–48, Jan. 2022, doi: 10.1089/dna.2021.0588.
- [4] S. Painuli, P. Semwal, R. Sharma, and S. Akash, 'Superbugs or multidrug resistant microbes: A new threat to the society', *Health Sci Rep*, vol. 6, no. 8, p. e1480, Aug. 2023, doi: 10.1002/hsr2.1480.

- [5] R. Han *et al.*, 'In Vitro Activity of KBP-7072 against 536 Acinetobacter baumannii Complex Isolates Collected in China', Microbiol Spectr, vol. 10, no. 1, pp. e01471-21, Feb. 2022, doi: 10.1128/spectrum.01471-21.
- [6] J. M. Colquhoun and P. N. Rather, 'Insights Into Mechanisms of Biofilm Formation in Acinetobacter baumannii and Implications for Uropathogenesis', *Front. Cell. Infect. Microbiol.*, vol. 10, p. 253, May 2020, doi: 10.3389/fcimb.2020.00253.
- [7] M. K. Jasim, Z. J. Hadi, H. A. A. Alsherees, and A. Annooz, 'Unmasking the Resistance: Detecting Carbapenem Genes in Acinetobacter baumannii Isolated from some Hospitals in Najaf and Baghdad', *Med.Sci.Jour.Adv.Res*, vol. 4, no. 2, pp. 101–111, Jul. 2023, doi: 10.46966/msjar.v4i2.127.
- [8] M. U. Munir, A. Ahmed, M. Usman, and S. Salman, 'Recent Advances in Nanotechnology-Aided Materials in Combating Microbial Resistance and Functioning as Antibiotics Substitutes', *IJN*, vol. Volume 15, pp. 7329–7358, Oct. 2020, doi: 10.2147/IJN.S265934.
- [9] B. Mubeen *et al.*, 'Nanotechnology as a Novel Approach in Combating Microbes Providing an Alternative to Antibiotics', *Antibiotics*, vol. 10, no. 12, p. 1473, Nov. 2021, doi: 10.3390/antibiotics10121473.
- [10] P. Beyer and S. Paulin, 'Priority pathogens and the antibiotic pipeline: an update', *Bull. World Health Organ.*, vol. 98, no. 3, pp. 151–151, Mar. 2020, doi: 10.2471/BLT.20.251751.
- [11] G. Angeles Flores, G. Cusumano, R. Venanzoni, and P. Angelini, 'Advancements in Antibacterial Therapy: Feature Papers', *Microorganisms*, vol. 13, no. 3, p. 557, Mar. 2025, doi: 10.3390/microorganisms13030557.
- [12] S. Gharpure and B. Ankamwar, 'Synthesis and Antimicrobial Properties of Zinc Oxide Nanoparticles', *j nanosci nanotechnol*, vol. 20, no. 10, pp. 5977–5996, Oct. 2020, doi: 10.1166/jnn.2020.18707.
- [13] Z. Marković *et al.*, 'Biocompatible Carbon Dots/Polyurethane Composites as Potential Agents for Combating Bacterial Biofilms: N-Doped Carbon Quantum Dots/Polyurethane and Gamma Ray-Modified Graphene Quantum Dots/Polyurethane Composites', *Pharmaceutics*, vol. 16, no. 12, p. 1565, Dec. 2024, doi: 10.3390/pharmaceutics16121565.
- [14] N. Parvin, S. W. Joo, and T. K. Mandal, 'Nanomaterial-Based Strategies to Combat Antibiotic Resistance: Mechanisms and Applications', *Antibiotics*, vol. 14, no. 2, p. 207, Feb. 2025, doi: 10.3390/antibiotics14020207.
- [15] H. Hemeg, 'Nanomaterials for alternative antibacterial therapy', IJN, vol. Volume 12, pp. 8211–8225, Nov. 2017, doi: 10.2147/IJN.S132163.
- [16] L. Mei et al., 'Two-dimensional nanomaterials beyond graphene for antibacterial applications: current progress and future perspectives', *Theranostics*, vol. 10, no. 2, pp. 757–781, 2020, doi: 10.7150/thno.39701.
- [17] V. Ahmad and M. O. Ansari, 'Antimicrobial Activity of Graphene-Based Nanocomposites: Synthesis, Characterization, and Their Applications for Human Welfare', *Nanomaterials*, vol. 12, no. 22, p. 4002, Nov. 2022, doi: 10.3390/nano12224002.
- [18] K. Arab, A. Jafari, and F. Shahi, 'The role of graphene quantum dots in cutting-edge medical therapies', *Polymers for Advanced Techs*, vol. 35, no. 9, p. e6571, Sep. 2024, doi: 10.1002/pat.6571.
- [19] A. T. S. Catanio *et al.*, 'Spectroscopic and photothermal characterization of graphene quantum dots for antimicrobial applications', *Journal of Applied Physics*, vol. 131, no. 15, p. 155102, Apr. 2022, doi: 10.1063/5.0084568.
- [20] W.-S. Kuo *et al.*, 'Nitrogen Functionalities of Amino-Functionalized Nitrogen-Doped Graphene Quantum Dots for Highly Efficient Enhancement of Antimicrobial Therapy to Eliminate Methicillin-Resistant Staphylococcus aureus and Utilization as a Contrast Agent', *IJMS*, vol. 22, no. 18, p. 9695, Sep. 2021, doi: 10.3390/ijms22189695.
- [21] P. Kadyan, P. Thillai Arasu, and S. K. Kataria, 'Graphene Quantum Dots: Green Synthesis, Characterization, and Antioxidant and Antimicrobial Potential', *International Journal of Biomaterials*, vol. 2024, pp. 1–11, Jan. 2024, doi: 10.1155/2024/2626006.
- [22] W.-S. Kuo, Y.-T. Shao, K.-S. Huang, T.-M. Chou, and C.-H. Yang, 'Antimicrobial Amino-Functionalized Nitrogen-Doped Graphene Quantum Dots for Eliminating Multidrug-Resistant Species in Dual-Modality Photodynamic Therapy and Bioimaging under Two-Photon Excitation', *ACS Appl. Mater. Interfaces*, vol. 10, no. 17, pp. 14438–14446, May 2018, doi: 10.1021/acsami.8b01429.
- [23] P. Sen, N. Nwahara, and T. Nyokong, 'Photodynamic antimicrobial activity of benzimidazole substituted phthalocyanine when conjugated to Nitrogen Doped Graphene Quantum Dots against *Staphylococcus aureus*', *Main Group Chemistry*, vol. 20, no. 2, pp. 175–191, Jul. 2021, doi: 10.3233/MGC-210030.

- [24] P. Lozovskis, E. Skrodenienė, V. Jankauskaitė, and A. Vitkauskienė, 'Effect of Graphene Oxide and Silver Nanoparticle Hybrid Composite on Acinetobacter baumannii Strains, Regarding Antibiotic Resistance and Prevalence of AMP-C Production', *Medicina*, vol. 59, no. 10, p. 1819, Oct. 2023, doi: 10.3390/medicina59101819.
- [25] Z. Ayed, S. Malhotra, G. Dobhal, and R. V. Goreham, 'Aptamer Conjugated Indium Phosphide Quantum Dots with a Zinc Sulphide Shell as Photoluminescent Labels for Acinetobacter baumannii', *Nanomaterials*, vol. 11, no. 12, p. 3317, Dec. 2021, doi: 10.3390/nano11123317.
- [26] 'Multidrug resistant (or antimicrobial-resistant) pathogens alternatives to new antibiotics?', *Swiss Med Wkly*, vol. 147, no. 4748, Nov. 2017, doi: 10.4414/smw.2017.14553.

